Cross-plane thermal properties of transition metal dichalcogenides

C. Muratore,[1,2,a)] V. Varshney,[2,3] J. J. Gengler,[2,4] J. J. Hu,[2,5] J. E. Bultman,[2,5] T. M. Smith,[6] P. J. Shamberger,[2] B. Qiu,[7] X. Ruan,[7] A. K. Roy,[2] and A. A. Voevodin[2]
[1]*Department of Chemical and Materials Engineering, University of Dayton, Dayton, Ohio 45469, USA*
[2]*Materials and Manufacturing Directorate, Air Force Research Laboratory, Wright-Patterson AFB, Ohio 45433, USA*
[3]*Universal Technology Corporation, Dayton, Ohio 45432, USA*
[4]*Spectral Energies LLC, Dayton, Ohio 45431, USA*
[5]*University of Dayton Research Institute, Dayton, Ohio 45469, USA*
[6]*Department of Materials Science and Engineering, Ohio State University, Columbus, Ohio 43210, USA*
[7]*Department of Mechanical Engineering and Birck Nanotechnology Center, Purdue University, West Lafayette, Indiana 47907, USA*

(Received 5 December 2012; accepted 7 February 2013; published online 26 February 2013)

In this work, we explore the thermal properties of hexagonal transition metal dichalcogenide compounds with different average atomic masses but equivalent microstructures. Thermal conductivity values of sputtered thin films were compared to bulk crystals. The comparison revealed a >10 fold reduction in thin film thermal conductivity. Structural analysis of the films revealed a turbostratic structure with domain sizes on the order of 5–10 nm. Estimates of phonon scattering lengths at domain boundaries based on computationally derived group velocities were consistent with the observed film microstructure, and accounted for the reduction in thermal conductivity compared to values for bulk crystals. © *2013 American Institute of Physics*. [http://dx.doi.org/10.1063/1.4793203]

Structure-property relationships for graphene are, in large part, appreciated in terms of the decades-old understanding of its three dimensional (3D) analog, graphite.[1,2] As two dimensional (2D) alternatives to graphene such as MoS_2 and other few-layer transition metal dichalcogenide (TMD) compounds are being explored for energy conversion, electronic device applications[3–5] or superlubricity in nanomachines,[6] our lack of understanding demands investigation of the structure-property relationships for these materials in order to accelerate the progress of their development. In particular, the thermal properties of 2D materials will have a strong influence on their selection for nanoscale electronic devices, which are likely to demonstrate thermally limited performance.[7] Here, we focus on thermal properties of bulk (single crystal) and thin film (~50 atomic layers) TMD materials with hexagonal structures, which are expected to have significantly lower in-plane and out-of-plane thermal conductivity than graphite.

Among several theoretical methods for predicting thermal conductivity, the Slack equation presents a simple framework that has been applied to several classes of non-metals with inputs of readily available materials properties, such as average atomic mass ($\overline{M}$) and Debye temperature (θ_D). The equation has previously been presented in different forms,[8–12] including

$$\kappa = \frac{B\overline{M}\delta{\theta_D}^3}{T{\gamma_G}^2 N^{2/3}}, \quad (1)$$

where δ^3 corresponds to average volume per atom, N is the number of atoms per unit cell, T is temperature, γ_G is the Grüneisen parameter,[9] and B is an amalgam of physical constants equivalent to 3.1×10^{-6} (with κ units in $W\,m^{-1}\,K^{-1}$, $\overline{M}$ in atomic mass units, T in Kelvin, and δ in Å). Although the average mass of the atoms comprising a material plays a linear role in predicted thermal conductivity, the Debye temperature is generally inversely proportional to average atomic mass thus making a stronger contribution to the predicted value of κ. Based on the Slack equation, hexagonal TMD compounds should, in general, possess very low thermal conductivity due to their high mass (high $\overline{M}$), atomic complexity (high N and γ_G) and weak bonding (high γ_G). In this study, experiments and first principles calculations were conducted to evaluate the predictive capability of the Slack equation for TMD materials over a broad range of atomic masses (and therefore Debye temperatures) and to better understand thermal transport in bulk and thin film forms of potentially useful 2D materials.

Thin films were processed in an ultra-high vacuum chamber with a base pressure of $<5 \times 10^{-9}$ Torr and were magnetron sputtered from pure (>99.9%) compound target materials. In all cases, substrates were polycrystalline Inconel 718 nickel superalloy disks that were electrically grounded and heated to 300 °C for degassing and deposition. The presence of nickel and chromium in the substrate aided the basal plane orientation of the films, as reported by other authors,[13,14] and evidenced by mixed 002/001 orientation for films grown on Si wafers subjected to identical processing conditions. Film purity was evaluated with an *in vacuuo* x-ray photoelectron spectroscopy (XPS) system in line with the processing chamber. No oxygen was detected, and the films appeared to be stoichiometric within approximately 2 atomic % (compositional resolution of the system). A set of freshly deposited films under identical conditions were immediately coated with a 70 nm layer of aluminum (Al) without breaking vacuum to avoid atmospheric exposure of the film surfaces

a)Author to whom correspondence should be addressed. Electronic mail: christophermuratore@hotmail.com.

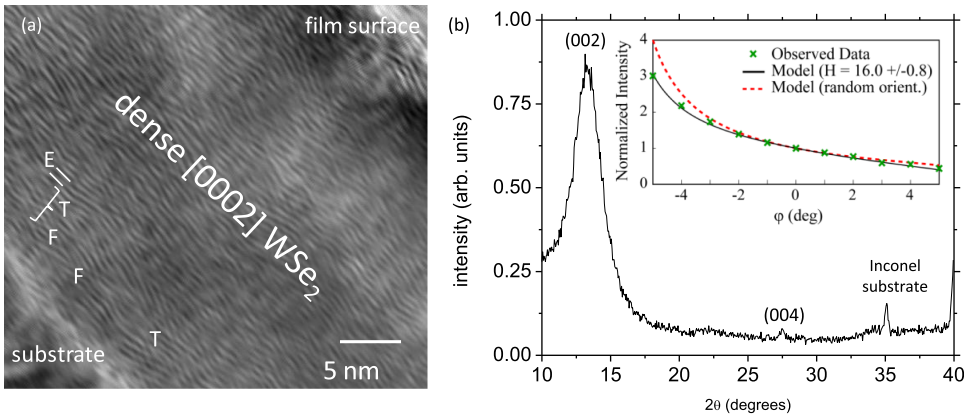

FIG. 1. (a) Transmission electron micrograph of WSe_2 film. Examples of fork (F), termination (T), and expansion (E) defects are called out. (b) X-ray diffractogram showing broad 002 peak, with rocking curve analysis in the inset.

during handling and storage, which had been shown in prior work to affect thermal conductivity values.[15] The aluminum also served as a protective layer during transmission electron microscopy (TEM) sample preparation of the films and as a transducer for thermal conductivity measurements by the time domain thermoreflectance (TDTR) technique. Aluminum was also applied to the bulk sample of MoS_2 investigated in the current work, which was obtained from a geologic specimen.

The structure and orientation of the Al-coated films were characterized by TEM of film cross-sections prepared with a focused ion beam (FIB), wide-angle x-ray diffraction and quantitative rocking curve analysis. A representative micrograph for the WSe_2 film is shown in Fig. 1(a)—the structure of all examined films looked similar, with thicknesses of $30\,\text{nm} \pm 5\,\text{nm}$ and equivalent "domain" sizes of approximately 5–10 nm. All films were also characterized by frequent atomic-scale defects, such as expanded atomic planes (E), fork defects (F), and termination defects (T) (as labeled on the figure). What we refer to as "domains" are simply collections of defects that appear to separate one region of the cross-section from another. These atomic-scale defects result in broadening of the 002 diffraction peak (shown for WS_2 in Fig. 1(b) as an example), in agreement with previously reported studies on TMD films.[16] The TEM micrographs of the films reveal a distinctive turbostratic structure, with domains of aligned basal planes that are approximately parallel to the film surface, but rotated about the thin film sample normal (n_s) with some small offset angle (ϕ) between n_s and n_c (crystal basal plane normal). Quantitative rocking-curve analysis following the method of Toraya *et al.* was consistent with the qualitative TEM results, indicating Gaussian distributions of ϕ with full width at half-maximum (FWHM) on the order of $\sim 15°$.[17] The inset to Fig. 1(b) demonstrates the case for WS_2 which is fit with a FWHM of $16.0° \pm 0.8°$ degrees within a 95% confidence level.

The thermal conductivity of bulk and thin film TMD materials was measured by a femtosecond TDTR method, as described in detail elsewhere.[18–20] In principle, TDTR is a laser-based approach to measuring thermal properties of materials by monitoring time-resolved, temperature-induced changes in optical reflectivity. Due to the substantial aspect ratio of laser spot size to thermal penetration depth, the TDTR measurements are selectively sensitive to one-dimensional thermal transport properties perpendicular to the sample surface (i.e., in the cross-plane direction). The TDTR values are shown in comparison to values calculated using the Slack equation, by plotting against its numerator (Fig. 2), in the manner similar to Ref. 12. The Debye temperatures used for each material were obtained from the literature.[21–23] The Grünheisen parameter was estimated at 2, which is a reasonable value for layered materials characterized by weak van der Waals bonding in the cross-plane direction.[9,11] Note that the measured thermal conductivity values for all studied thin film TMDs fall on a line that is offset from the values predicted by the Slack equation and the measurement of the bulk crystals (the data for bulk WSe_2 were measured in Ref. 24). The offset reveals an approximate order of magnitude reduction in thermal conductivity of the thin film TMD materials.

To identify the role of defects and nanostructure on the reduced values of thermal conductivity in thin films, analysis by the Matthiessen rule[9] for thermal resistances in series was considered. This rule provides a framework to predict effective thermal resistance (or conductivity) for materials in which multiple phonon scattering mechanisms are involved. While the Slack equation (Eq. (1)) takes only phonon-phonon scattering into account for estimating thermal conductivity (which is an appropriate model for the semiconducting bulk TMD studied here), the contribution of phonon scattering at domain boundaries to thermal conductivity is neglected. Boundary effects can be incorporated into the calculation by introducing a term based on the time between scattering

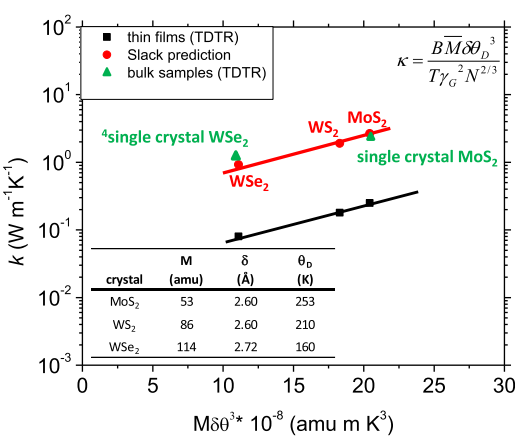

FIG. 2. Measured thermal conductivity for TMD bulk (green triangles) and thin film (black squares) materials compared to values calculated using the Slack equation (red circles). The inset table shows values for parameters used in Slack equation as obtained in the literature. The lines are least square linear fit to data points.

events. In such cases, the effective thermal conductivity can be written as:

$$\frac{1}{k_{measured}} = \frac{1}{k_{p-pscatter}} + \frac{1}{k_{\text{int}\,scatter}} = \frac{1}{k_{Slack}} + \frac{1}{\frac{1}{3}(C_v u_p{}^2 \tau_{\text{int}\,scatter})}, \quad (2)$$

where C_v is the volumetric heat capacity, u_p is the phonon group velocity, and τ is the relaxation time (time between phonon scattering events at interfaces), which is equivalent to the distance between scattering interfaces (L, which is also equivalent to average domain size) divided by group velocity ($\tau = L/u_p$). For such anisotropic materials, a more sophisticated approach would be to use the mode-resolved group velocity and relaxation time which depend on the phonon frequency and wave vector in the first Brillouin zone.[25] However, the structure of our material is very complicated, and mode-resolved phonon relaxation times are not available in the literature. Hence, we have used this "gray" approach, which assumes a single effective phonon group velocity and relaxation time, to interpret our experimental data. The group velocity for acoustic phonon modes in perfect crystals can be obtained from the slope of the appropriate dispersion curve near the center of the Brillouin zone. Of the materials considered in this study, phonon dispersion curves could only be found for MoS_2 in the reported literature.[26]

As phonon group velocity is a key parameter to be incorporated in Eq. (2) for the estimation of distance between interfacial scattering sites (or scattering length), the evaluation of the group velocities of different studied TMD systems is necessary. In order to do so, first principles density functional theory (DFT) calculations were performed to investigate the crystalline structure and predict dispersion curves for MoS_2, WS_2, and WSe_2. The open-source ABINIT package[27,28] was employed to carry out all the DFT calculations within the local density approximation (LDA).[29] Among available pseudo-potentials, the norm-conserving Troullier-Martins (TM) pseudo-potentials for MoS_2, WS_2, and WSe_2 were found to produce best agreement with experiments in cross-plane lattice constants.[30] In addition, the shifted $12 \times 12 \times 4$ Monkhorst-Pack grid and a plane-wave cutoff of 60 Hartrees (Ha) led to convergence in the self-consistent (SCF) ground state energies and optimized lattice constants for all cases. The Broyden-Fletcher-Goldfarb-Shanno (BFGS) minimization was performed for geometry optimization until the residual forces on each atom were below 10^{-6} Ha/Bohr. The optimized lattice parameters are shown in Table I. Based on the optimized lattice structures, the phonon dispersions were obtained by solving the generalized eigenvalue problem set by the dynamical matrix, calculated using the density functional perturbation theory (DFPT) as implemented in ABINIT package.

TABLE I. DFT predicted lattice parameters of MoS_2, WS_2, and WSe_2 and their comparison with reported experimental literature.

	a (Å)		c (Å)	
Compound	Predicted	Measured	Predicted	Measured
MoS_2	3.20	3.15[a]	12.13	12.30
WS_2	3.18	3.15[b]	12.21	12.32
WSe_2	3.28	3.28[b]	12.73	12.96

[a]R. G. Dickinson and L. Pauling, J. Am. Cer. Soc. **45**, 1466 (1923).
[b]W. J. Schutte, J. L. de Boer, and F. Jellinek, J. Solid State Chem. **70**, 207 (1987).

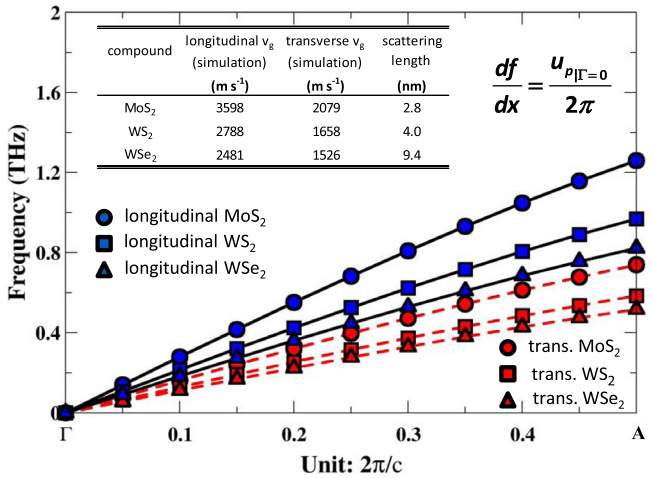

FIG. 3. Acoustic phonon dispersion curves for TMD materials considered in this study along (002) direction: blue symbols (solid lines) are for longitudinal modes for MoS_2 (circles), WS_2 (squares), and WSe_2 (triangles), red (dashed lines) for transverse with same compound identification scheme. Calculated group velocities for each material are inset.

The predicted dispersion curves for transverse (ZA) and longitudinal (LA) acoustic phonons along (002) direction are shown in Fig. 3. A table of velocities estimated from the calculated dispersion curves is shown as an inset for the investigated TMD materials. We should point out that the predicted velocities for MoS_2 and WSe_2 are consistent with values reported in the literature.[24,26] For calculating effective domain size (L), we assumed, as in Ref. 24, that the elastic moduli of the thin films had values that were approximately half of those of the bulk crystals. Therefore, the group velocities (u_p) were reduced to $\frac{u_{predicted}}{\sqrt{2}}$. In addition, the longitudinal and transverse velocities along (002) direction were weighted to account for an estimated contribution of each mode to heat conduction (two transverse, and one longitudinal) as follows:

$$u_p = \frac{u_l + 2u_t}{3}.$$

We assumed that domain length was isotropic and scattered both modes with equivalent frequency. The table in Fig. 3 also shows the calculated distance between interfacial scattering sites (or scattering length, L) necessary to reduce the predicted or bulk crystal thermal conductivity for an ordered 002 crystal (red line in Fig. 2), to the value measured for the thin films characterized in this work (black line in Fig. 2). Comparison of the calculated scattering length to the domain size in Fig. 1 suggests that interfacial scattering does indeed account greatly for the reduced value of thermal conductivity, illustrating the impact of nanostructural defects on thermal properties of TMD films.

In conclusion, we have used magnetron sputtering to produce thin TMD films with highly defective turbostratic

structures. Comparison of bulk and thin film thermal conductivity shows a structure dependence of a factor of >10. To explore the nature of this reduction, we evaluated the effect of domain size on phonon scattering. Using the Matthiessen framework of thermal resistances in series, it was demonstrated that phonon scattering at the domain boundaries greatly influences thermal transport characteristics along cross-plane direction in layered TMDs. This work provides insight on materials selection and processing for 2D materials applications where thermal properties are crucial, as in power transistors or nanoscale mechanical assemblies with contacts in relative motion.

The authors are grateful for funding from the Thermal Sciences Program of the Air Force Office of Scientific Research for financial support of this work. X.R. was sponsored by an Air Force Research Laboratory Summer Faculty Fellowship. C.M. would like to thank Professor Tim Fisher at Purdue and Professor David Cahill at UIUC for insightful discussions and guidance.

[1]C. A. Klein and M. G. Holland, Phys. Rev. **136**, A575–A590 (1964).
[2]G. A. Slack, Phys. Rev. **127**, 694 (1962).
[3]K.-K. Liu, W. Zhang, Y.-H. Lee, Y.-C. Lin, M.-T. Chang, C.-Y. Su, C.-S. Chang, H. Li, Y. Shi, H. Zhang, C.-S. Lai, and L.-J. Li, Nano Lett. **12**, 1538 (2012).
[4]K. F. Mak, C. Lee, J. Hone, J. Shan, and T. F. Heinz, Phys. Rev. Lett. **105**, 136805 (2010).
[5]Y. Yoon, K. Ganapathi, and S. Salahuddin, Nano Lett. **11**, 3768 (2011).
[6]Z. Liu, J. Yang, F. Grey, J. Z. Liu, Y. Liu, Y. Wang, Y. Yang, Y. Cheng, and Q. Zheng, Phys. Rev. Lett. **108**, 205503 (2012).
[7]D. G. Cahill, W. K. Ford, K. E. Goodson, G. D. Mahan, A. Majumdar, H. J. Maris, R. Merlin, and S. R. Philpot, J. Appl. Phys. **93**, 793 (2003).
[8]D. R. Clarke, Surf. Coat. Technol. **163-164**, 67 (2003).
[9]M. Kaviany, *Heat Transfer Physics* (Cambridge University Press, 2008).
[10]D. T. Morelli and G. A. Slack, in *High Thermal Conductivity Materials*, edited by S. L. Shinde and J. S. Goela (Springer, New York, 2006), Chap. 2, p. 37.
[11]D. T. Morelli, V. Jovovic, and J. P. Heremans, Phys. Rev. Lett. **101**, 035901 (2008).
[12]G. A. Slack, J. Phys. Chem. Solids **34**, 321 (1973).
[13]O. Lignier, G. Couturier, and J. Salardenne, Thin Solid Films **338**, 75 (1999).
[14]G. Salitra, G. Hodes, E. Klein, and R. Tenne, Thin Solid Films **245**, 180 (1994).
[15]R. C. McLaren, M.S. thesis, University of Illinois at Urbana-Champaign, 2009.
[16]D. N. Dunn, L. E. Seitzman, and I. L. Singer, J. Mater. Res. **12**, 1191 (1997).
[17]H. Toraya, H. Hibino, T. Ida, and N. Kuwano, J. Appl. Cryst. **36**, 890 (2003).
[18]D. G. Cahill, Rev. Sci. Instrum. **75**, 5119 (2004).
[19]J. J. Gengler, C. Muratore, A. K. Roy, J. J. Hu, A. A. Voevodin, S. Roy, and J. R. Gord, Compos. Sci. Technol. **70**(14), 2117 (2010).
[20]J. J. Gengler, S. Roy, J. G. Jones, and J. R. Gord, Meas. Sci. Technol. **23**, 055205 (2012).
[21]S. Y. Hu, Y. C. Lee, J. L. Shen, K. W. Chen, and Y. S. Huang, Phys. Status Solidi (a) **204**, 2389 (2007).
[22]K. T. Park, M. Richards-Babb, J. S. Hess, J. Weiss, and K. Klier, Phys. Rev. B **54**, 5471 (1996).
[23]S. A. Wender and N. Hershkowitz, Phys. Rev. B **8**, 4901 (1973).
[24]C. Chiritescu, D. G. Cahill, N. Nguyen, D. Johnson, A. Bodapati, P. Keblinski, and P. Zschack, Science **315**, 351 (2007).
[25]Y. Wang, B. Qiu, A. J. H. McGaughey, X. Ruan, and X. Xu, "Mode-wise thermal conductivity of bismuth telluride," J. Heat Transfer (in press).
[26]N. Wakabayashi, H. G. Smith, and R. M. Nicklow, Phys. Rev. B **12**, 659 (1975).
[27]X. Gonze, G.-M. Rignanese, M. Verstraete, J.-M. Beuken, Y. Pouillon, R. Caracas, F. Jolliet, M. Torrent, G. Zerah, M. Mikami, Ph. Ghosez, M. Veithen, J.-Y. Raty, V. Olevano, and F. Bruneval, Z. Kristallogr. **220**, 558 (2005).
[28]X. Gonze, B. Amadon, P.-M. Anglade, J.-M. Beuken, F. Bottin, P. Boulanger, F. Bruneval, D. Caliste, R. Caracas, M. Cote, T. Deutsch, L. Genovese, and Ph. Ghosez, Comput. Phys. Commun. **180**, 2582 (2009).
[29]W. Kohn and L. J. Sham, Phys. Rev. **140**, A1133 (1965).
[30]N. Troullier and J. L. Martins, Phys. Rev. B **43**, 1993 (1991).